Microwave Spectrum, Structure, and Quantum Chemical Studies of a Compound of Potential Astrochemical and Astrobiological Interest: *Z*-3-Amino-2-propenenitrile

Eva Askeland,[†] Harald Møllendal,*[,†] Einar Uggerud,[†] Jean-Claude Guillemin,[‡] Juan-Ramon Aviles Moreno,[§] Jean Demaison,[§] and Thérèse R. Huet[§]

Department of Chemistry, University of Oslo, Post Office Box 1033 Blindern, NO-0315 Oslo, Norway, UMR CNRS 6226, Ecole Nationale Supérieure de Chimie de Rennes, F-35700 Rennes, France, and Laboratoire de Physique des Lasers, Atomes, et Molécules, UMR CNRS 8523, Université de Lille I, Bat. P5, F-59655 Villeneuve d'Ascq, France

Received: July 3, 2006; In Final Form: August 25, 2006

Z-3-Amino-2-propenenitrile, $H_2NCH{=}CHCN$, a compound of astrochemical and astrobiological interest, has been studied by Stark and Fourier transform microwave spectroscopy along with eight of its isotopologues; the synthesis of five of these are reported. The spectra of the ground vibrational state and of three vibrationally excited states belonging to the two lowest normal modes were assigned for the parent species, whereas the ground states were assigned for the isotopologues. The frequency of the lowest in-plane bending fundamental vibration was determined to be 152(20) cm^{-1} and the frequency of the lowest out-of-plane fundamental mode was found to be 176(20) cm^{-1} by relative intensity measurements. A delicate problem is whether this compound is planar or slightly nonplanar. It was found that the rotational constants of the nine species cannot be used to conclude definitely whether the molecule is planar or not. The experimental dipole moment is $\mu_a = 16.45(12)$, $\mu_b = 2.86(6)$, $\mu_c = 0$ (assumed), and $\mu_{tot.} = 16.70(12) \times 10^{-30}$ C m [5.01(4) D]. The quadrupole coupling constants of the two nitrogen nuclei are $\chi_{aa} = -1.4917(21)$ and $\chi_{cc} = 1.5644(24)$ MHz for the nitrogen atom of the cyano group and $\chi_{aa} = 1.7262(18)$ and $\chi_{cc} = -4.0591(17)$ MHz for the nitrogen atom of the amino group. Extensive quantum-chemical calculations have been performed, and the results obtained from these calculations have been compared with the experimental values. The equilibrium structures of vinylamine, vinyl cyanide, and *Z*-3-amino-2-propenenitrile have been calculated. These calculations have established that the equilibrium structure of the title compound is definitely nonplanar. However, the MP2/VQZ energy difference between the planar and nonplanar forms is small, only −423 J/mol. *Z*-Amino-2-propenenitrile and *E*-3-amino-2-propenenitrile are formed simply by mixing ammonia and cyanoacetylene at room temperature. A plausible reaction path has been modeled. G3 calculations indicate that the enthalpy (298.15 K, 1 atm) of the transition state is about 130 kJ/mol higher than the sum of the enthalpies of the reactants ammonia and cyanoacetylene. This energy difference is comparatively high, which indicates that both *E*- and *Z*-3-aminopropenenitrile are not likely to be formed in the gas phase in cold interstellar clouds via a collision between ammonia and cyanoacetylene. An alternative reaction between protonated cyanoacetylene ($H{-}C{\equiv}C{-}C{\equiv}NH^+$) and ammonia is predicted to have a much lower activation energy than the reaction between the neutral molecules. Although protonated *E*- and *Z*-3-aminopropenenitrile in principle may be formed this way, it is more likely that a collision between NH_3 and $H{-}C{\equiv}C{-}C{\equiv}NH^+$ leads to $NH_4^+$and $H{-}C{\equiv}C{-}C{\equiv}N$.

Introduction

It was pointed out in a very recent study[1] that the two isomers of aminopropenenitrile, *Z*- and *E*-3-amino-2-propenenitrile ($H_2N{-}CH{=}CH{-}C{\equiv}N$), might exist in the interstellar medium, in comets, and in the atmospheres of planets, and they may also have existed on primitive Earth. The reason for this suggestion is that this compound is readily formed in a 1:1 *Z:E* mixture at room temperature in the gas phase[2] or in solution[3] simply by mixing cyanoacetylene ($HC{\equiv}C{-}C{\equiv}N$) and ammonia (NH_3), two compounds that are prevalent in the Universe. The reactant cyanoacetylene has, for example, been observed in interstellar space,[4,5] in comets[6] and in the atmosphere of Titan.[7,8] The other precursor, ammonia, is also a ubiquitous extraterrestrial molecule.[9,10] Moreover, Eschenmoser and co-workers[3,11−15] have pointed out that aminopropenenitrile may have played a role in prebiotic chemistry in the formation of carbohydrates and amino acids.

Previous investigations[1,3] of the title compound have shown that the *Z:E* ratio, which is roughly 1:1 in the reaction mixture, increases to about 20:1 after distillation in vacuo. Distilled samples were used in the most recent study,[1] in which the infrared (IR) spectrum of aminopropenenitrile was investigated in the 500−4000 cm^{-1} spectral region in the gas and liquid phases. The spectrum of only the major *Z*-isomer was observed in the gaseous state, whereas the IR spectra of both isomers were observed in the liquid. Quantum-chemical calculations of several physical properties were also perfomed.[1] G2[16] and

* Corresponding author. Telephone: +47 2285 5674. Fax: +47 2285 5441. E-mail: harald.mollendal@kjemi.uio.no.
[†] University of Oslo.
[‡] Ecole Nationale Supérieure de Chimie de Rennes.
[§] Université de Lille I.

10.1021/jp064152d CCC: $33.50
Published on Web 11/01/2006

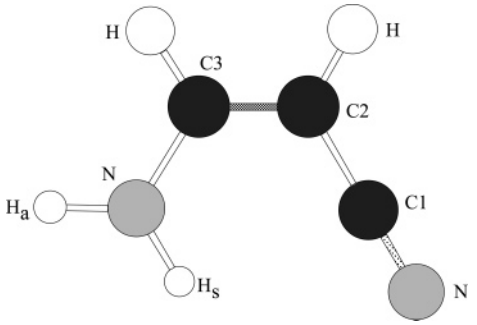

Figure 1. Model of *Z*-3-amino-2-propenenitrile (APN) with atom numbering. Evidence is presented to show that the compound has a slightly nonplanar equilibrium conformation.

density functional theory calculations employing the B3LYP[17,18] procedure with the 6-311+G(3df,2p) basis set both predict the *Z*-isomer to be approximately 8.0 kJ/mol (Gibbs energy difference at 100 K) more stable than the *E*-isomer.[1] It was also found that a rotation about the double bond is the likely thermal interconversion path between the *Z*- and the *E*-isomers, whereas this isomerization may occur via an enamine−imine tautomerism path in a basic solution. The transition state for the thermal interconversion was predicted to lie approximately 215 kJ/mol above the energy of the *Z*-isomer.[1]

Nitriles are among the most commonly reported interstellar organic molecules and have been identified in a number of sources in interstellar space.[19,20] It is considered likely that nitriles containing an amino group have played a key role in the formation of amino acids, which have been found in certain meteorites.[20] A radio astronomical search for the *Z*-isomer of the title compound in the Sagittarius B2 (N) interstellar cloud has recently been performed.[21] This search concentrated on identifying microwave (MW) signals from this source that coincide with the MW transitions presented in this work, but no identifications could be made.[21]

The likely formation of extraterrestrial aminopropenenitrile and its potentially prebiotic role were the main motivations for undertaking the present MW and quantum chemical study of *Z*-3-amino-2-propenenitrile, henceforth called APN. A model with atom numbering is depicted in Figure 1.

The MW spectrum of APN was investigated because such spectra are very useful for identifying molecules in interstellar space, in the gas jets of comets, and in the atmospheres of planets.[19] Both Stark-modulated (Oslo) and Fourier transform (Lille) MW spectroscopy have been employed, since these techniques yield complementary information.

The MW spectra of several isotopologues have also been investigated because they should be of interest in a possible future identification of APN in the Universe. Another reason for studying isotopologues has been that the rotational constants obtained from their MW spectra can be used to derive information about the structure of this compound.

On aspect of the structure of APN is whether this molecule is exactly planar. Interestingly, the related molecule vinylamine ($H_2C{=}CHNH_2$) is definitely nonplanar.[22−24] The title compound thus offers the possibility of investigating the effect the nitrile substituent may have on the structural properties. The molecular dipole moment and the nuclear quadrupole coupling constants of the two nitrogen nuclei are also important for the determination of the molecular symmetry and bonding properties and have therefore been investigated in the course of this study.

Quantum-chemical calculations at high levels of theory have also been performed primarily to assist in the assignment procedure, to predict an accurate equilibrium structure, dipole moment, and quadrupole coupling constants, and to model the gas-phase reaction between ammonia and cyanoacetylene forming 3-aminopropenenitrile.

SCHEME 1

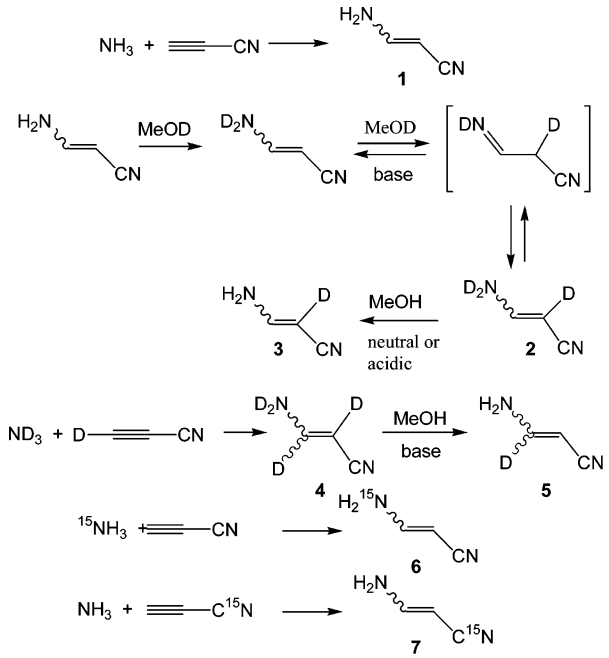

Experimental Section

Synthesis of 3-Amino-2-propenenitrile and Its Isotopologues. 3-Amino-2-propenenitrile has been synthesized by mixing gaseous ammonia and cyanoacetylene.[1] The preparations of cyanoacetylene, cyanoacetylene-*d*, and cyanoacetylene-^{15}N are given in the Supporting Information. ^{15}N-enriched ammonia was used to synthesize the ^{15}N species. The syntheses of the 2- and 3-deuterated derivatives were more difficult to perform. This work was complicated by the fast exchange between the hydrogen(s) or deuterium(s) of ammonia and cyanoacetylene. It has already been reported that the thermal $E \rightarrow Z$ isomerization does not occur via an enamine−imine tautomerism.[1] However, such tautomerism occurs in the presence of a base. Thus a 95:5 *Z*:*E* ratio of aminopropenenitrile led to a 1:1 *Z*:*E* ratio by addition of small amounts of a base such as sodium hydroxide, triethylamine, or 1,8-diazabicyclo[5,4,0]undec-7-ene (DBU).[1] We used this property to prepare the two deuterated derivatives. All these results are summarized in Scheme 1.

(*Z*+*E*)-3-Amino-d_2-2-deuterio-2-propenenitrile (2). (*Z*+*E*)-3-Amino-2-propenenitrile (**1**; 1.36 g, 20 mmol) was introduced in a flask with 5 mL of methanol-*d*. A few drops of triethylamine were added. After 2 h of stirring at room temperature, the low-boiling compounds were evacuated in vacuo. This sequence was repeated by addition of methanol-*d* and triethylamine. The crude compound **2** in a 1:1 *Z*:*E* ratio was purified by distillation in vacuo ($bp_{0.1}$, 63 °C) to give **2** (95:5 *Z*:*E* ratio) in a 78% yield (1.10 g). Isot pur > 97%. (***Z***) ^{1}H NMR ($CDCl_3$, 400 MHz): δ 6.78 (t, 1H, $^3J_{HD}$ < 1 Hz, CH−N). ^{13}C NMR ($CDCl_3$, 100 MHz): δ 63.1 ($^1J_{CD}$ = 27.3 Hz, CH−CN); 118.4 (CN); 149.5 (CH−N). (***E***) ^{1}H NMR ($CDCl_3$, 400 MHz): δ 6.98 (t, 1H, $^3J_{HD}$ = 1.9 Hz, CH−N). ^{13}C NMR ($CDCl_3$, 100 MHz): δ 65.2 ($^1J_{CD}$ = 27.3 Hz, CH−CN); 122.2 (CN); 151.0 (CH−N). IR (neat; ν, cm^{-1}): 2529 (ν_{N-D}) (m), 2189 (ν_{CN}) (s), 1618 ($\nu_{C=C}$) (s), 1308 (s), 977 (s). HRMS. Calcd for $C_3H_1D_3N_2$: 71.0563. Found: 71.0561.

(*Z*+*E*)-3-Amino-2-deuterio-2-propenenitrile (3). (*Z*+*E*)-3-Amino-d_2-2-deuterio-2-propenenitrile **2** (710 mg, 10 mmol) was introduced in a flask with 5 mL of methanol. After 5 min of stirring, methanol was removed in vacuo. Compound **3** purified by distillation in vacuo ($bp_{0.1}$, 63 °C) was obtained in a 85% yield (587 mg). Isot pur > 94%. (***Z***) ^{1}H NMR ($CDCl_3$, 400 MHz): δ 4.96 (s brd, 2H, NH_2); 6.77 (tt, 1H, $^3J_{HH}$ = 10.6 Hz,$^3J_{HD}$ = 1.3 Hz, CH−N). ^{13}C NMR ($CDCl_3$, 100 MHz): δ 62.6 ($^1J_{CD}$ = 27.1 Hz, CH−CN); 118.5 ($^2J_{CD}$ = 12.0 Hz, CN); 149.9 (CH−N). (**E**) ^{1}H NMR ($CDCl_3$, 400 MHz): δ 4.96 (s brd, 2H, NH_2); 6.92 (t, 1H, $^3J_{HH}$ = 10.7 Hz,$^3J_{HD}$ = 1.9 Hz, CH−N). ^{13}C NMR ($CDCl_3$, 100 MHz): δ 65.2 ($^1J_{CD}$ = 25.6 Hz, CH−CN); 121.4 (CN); 151.2 (CH−N).

(*Z*+*E*)-3-Amino-d_2-2,3-deuterio-2-propenenitrile (4). Gaseous ammonia-d_3 was mixed with cyanoacetylene-*d*, as reported for **1**[1] (Supporting Information), and the product was purified by distillation in vacuo (yield: 80%). (***Z***) ^{13}C NMR ($CDCl_3$, 100 MHz): δ 61.4 ($^1J_{CD}$ = 27.3 Hz, CH−CN); 118.8 (CN); 149.8 ($^1J_{CD}$ = 25.7 Hz, CH−N). (***E***) ^{13}C NMR ($CDCl_3$, 100 MHz): δ 63.1 ($^1J_{CD}$ = 26.0 Hz, CH−CN); 121.6 (CN); 151.0 ($^1J_{CD}$ = 25.8 Hz, CH−N).

(*Z*+*E*)-3-Amino-3-deuterio-2-propenenitrile (5). Compound **4** (720 mg, 10 mmol) was introduced in a flask with methanol (10 mL), and a few drops of triethylamine were added. After 2 h of stirring at room temperature, the low-boiling compounds were removed in vacuo and the (*Z*+*E*)-3-amino-3-deuterio-2-propenenitrile (**4**) was purified by distillation ($bp_{0.1}$, 63 °C). Yield: 566 mg, 8.2 mmol, 82%. Isot pur > 94%. (***Z***) ^{1}H NMR ($CDCl_3$, 400 MHz): δ 3.97 (s, 1H, CH−CN); 4.86 (s brd, 2H, NH_2). ^{13}C NMR ($CDCl_3$, 100 MHz): δ 63.0 (CH−CN); 118.5 (CN); 149.8 ($^1J_{CD}$ = 25.7 Hz, CH−N). (***E***) ^{1}H NMR ($CDCl_3$, 400 MHz): δ 4.27 (s, 1H, CH−CN); 4.52 (s brd, 2H, NH_2). ^{13}C NMR ($CDCl_3$, 100 MHz): δ 65.5 (CH−CN); 121.4 (CN); 151.0 ($^1J_{CD}$ = 25.7 Hz, CH−N).

(*Z*+*E*)-3-Amino-^{15}N-2-propenenitrile (6).[25] This compound was prepared in a 80% yield by the synthesis described for **1**[1] (Supporting Information) using ammonia-^{15}N and cyanoacetylene. ^{15}N NMR ($CDCl_3$, 500.1 MHz): δ −302.0 ((***E***), $^1J_{NH}$ = 90.5 Hz); −301.0 ((***Z***), $^1J_{NH}$ = 92 Hz).

(*Z*+*E*)-3-Amino-2-propenenitrile-^{15}N (7).[25] This compound was prepared in a 80% yield by the synthesis described for **1**[1] using ammonia and cyanoacetylene-^{15}N. (***Z***) ^{13}C NMR ($CDCl_3$, 100 MHz): δ 61.4 (CH−CN); 118.9 ($^1J_{CN}$ = 17.6 Hz, CN); 150.5. (***E***) ^{13}C NMR ($CDCl_3$, 100 MHz): δ 63.7 (CH−CN), 122.0 ($^1J_{CN}$ = 18.4 Hz, CN); 151.8 (CH−N). ^{15}N NMR ($CDCl_3$, 500.1 MHz): δ −135.4 (***E***); −121.0 (***Z***).

***Z*-3-Amino-*d*-2-propenenitrile (8).** There are two rotamers in this case having the H−N−C−C chain of atoms in a syn-periplanar or in an anti-periplanar configuration, respectively. Both these species were produced by exchange between Z-3-amino-2-propenenitrile and heavy water in the MW cell. The cell was first conditioned with heavy water. Fumes of the APN were then introduced. The spectra of the syn-periplanar and anti-periplanar forms produced in this manner were each observed to have roughly 25% of the intensity of the spectrum of the pure parent species.

Stark Spectrometer Experiment. The MW spectrum of APN was studied at room temperature in the 10−80 GHz spectral region with the Stark spectrometer in Oslo. The main features of this spectrometer have been described elsewhere.[26,27]

Preliminary quantum-chemical calculations indicated that APN should have a dipole moment component along the *a*-principal inertial axis of about 17 × 10^{-30} C m [5 D] (see below). This should result in a comparatively strong MW spectrum. However, it turned out that it was problematic to obtain a sufficiently strong Stark spectrum for several reasons. The samples used in our experiments were synthesized in Rennes, but they had been distilled and transported to Oslo dissolved in dichloromethane. Most of the dichloromethane was first removed by distillation under reduced pressure, leaving behind a brown, viscous residue, which is obviously associated with polymeric material. Dichloromethane has a strong and rich MW spectrum, and it was essential to remove this volatile component completely in order to obtain the MW spectrum of APN. Pumping on the sample by simply using a diffusion pump was not sufficient. It was necessary to heat the sample vigorously with a heat gun while evacuating with a diffusion pump to remove the last dichloromethane completely. The upper part of the sample tube was cooled with dry ice during this operation in order to condense the sample, which contained more than 95% of the *Z*-isomer (APN) of aminopropenenitrile according to the NMR spectroscopy.[1] The measured vapor pressure of APN at room temperature was roughly of the order of 10−25 Pa. The observed spectrum was much weaker than expected for a molecule with a dipole moment of approximately 17 × 10^{-30} C m. It was therefore assumed that a major part of the vapor belongs to gaseous impurities, which were only partly identified. HC≡C−C≡N was searched for using both Stark and Fourier transform techniques but was not found. Ammonia was identified and is one impurity, but the vapor pressure indicated that there had to be additional impurities as well. It was also observed that the intensity of the spectrum diminished rather rapidly in the Stark experiment. It is assumed that this is due to a partial adsorption of the sample onto the cell walls, followed by the formation of polymerization products or similar reactions. The cell therefore had to be refilled frequently with fresh sample.

Microwave Fourier Transform Experiment. The spectrum of APN was recorded in the 4−20 GHz spectral range using the molecular jet microwave Fourier transform spectrometer in Lille.[28] A pure sample (not diluted in dichloromethane) was used in this experiment. No extensive searching for impurities was performed. The sample was heated at a temperature of 320 K and mixed with neon at a stagnation pressure of 1.5 bar. The gas was injected into the vacuum tank by means of a pulsed nozzle at a rate of 2 Hz to create a supersonic expansion with a rotational temperature of 1−2 K. The cell is a Fabry−Perot cavity of adjustable length, with a mode bandwidth of about 0.4 MHz. Molecules in the expansion were probed with 2 μs pulses of tunable MW radiation, and the free-induction decay occurring at each resonance frequency was detected and processed. This operation was then automatically repeated every 0.4 MHz in order to cover the desired frequency region. As the nozzle is inserted in the center of the fixed mirror of the Fabry−Perot cavity, the supersonic expansion is parallel to the MW axis of the cavity, and each transition is consequently divided into two Doppler components. The central frequency of each line was determined by averaging the frequencies of the two Doppler components after the transformation of 4096 data points in the time domain signal, leading to an accuracy of 2.4 kHz. The line width of a well-resolved line was 10 kHz.

Assignment of the MW Spectrum Using Stark Spectroscopy. Accurate predictions of the rotational constants and dipole moment components along the principal inertial axis are very useful when assigning MW spectra. It has been shown[29] that Møller−Plesset second-order perturbation calculations (MP2)[30] using a large basis set predict structures that are close to equilibrium structures. The approximate *equilibrium* rotational constants calculated from such structures should normally be

close (≈2%) to the *effective* rotational constants obtained from the MW spectra. The relatively large 6-311++G** basis set, which is of triple-ζ quality and includes diffuse functions, was employed in a MP2 calculation to predict rotational constants, Watson's quartic centrifugal distortion constants,[31] and dipole moment components along the principal inertial axes using the Gaussian 03 program.[32] The results of these predictions were $A = 12\,521$, $B = 3701$, and $C = 2861$ MHz for the rotational constants, $\Delta_J = 4.32$, $\Delta_{JK} = -31.2$, and $\Delta_K = 94.2$ kHz, $\delta_J = 1.41$ and $\delta_K = 7.96$ kHz for the quartic centrifugal distortion constants, and $\mu_a = 17.7$, $\mu_b = 3.7$, and $\mu_c = 2.8 \times 10^{-30}$ C m for the dipole moment components. APN is therefore predicted to be a near-prolate asymmetric top (Ray's asymmetry parameter,[33] $\kappa = -0.82$).

Searches were first made for the strong *a*-type R-branch transitions using these rotational and centrifugal distortion constants, because this dipole moment component is $\approx 17.7 \times 10^{-30}$ C m [5.2 D]. These lines were readily identified and analyzed employing Watson's Hamiltonian (*A* reduction I^r representation).[31] The assignments were also confirmed by their characteristic Stark effects.

In Watson's model, the rigid asymmetric rotor is described in the I^r representation by the $\hat{H}_R$ part of the Hamilitonian:

$$\hat{H}_R = \left[A - \frac{1}{2}(B+C)\right]\hat{J}_z^2 + \frac{1}{2}(B+C)\hat{J}^2 + \frac{1}{4}(B-C)(\hat{J}_+^2 + \hat{J}_-^2) \quad (1)$$

where *A*, *B*, and *C* are the rotational constants. The centrifugal distortion corrections were accounted for by Watson's *A*-reduced $\hat{H}_{CD}$ Hamiltonian:[31]

$$\hat{H}_{CD} = -\Delta_J\hat{J}^4 - \Delta_{JK}\hat{J}^2\hat{J}_z^2 - \Delta_K\hat{J}_z^4 - \delta_K[\hat{J}_z^2, \hat{J}_x^2 - \hat{J}_y^2]_+ - 2\delta_J\hat{J}^2(\hat{J}_x^2 - \hat{J}_y^2) \quad (2)$$

About 110 *a*-type R-branch transitions with the *J* principal quantum number between $J = 1$ and 13 were assigned this way and analyzed in a least-squares fit by Sørensen's ROTFIT program.[34] The transitions are listed in Table 1S in the Supporting Information. Searches were made for *b*- and *c*-type transitions, but these were not found. This was presumably because of the experimental problems mentioned above as well as much smaller *b*- and *c*-dipole moment components (see below), rendering them too weak to allow definite assignments to be made.

APN has two ^{14}N nuclei, which have spin = 1, and therefore a nuclear quadrupole moment. This results in a complicated hyperfine structure caused by quadrupole coupling of the spin angular moments of the two nuclei with the rotation. The resolution of the Stark spectrometer is not sufficiently high to resolve the resulting hyperfine splittings, which produced broad lines that in many cases had a skew shape instead of the normal symmetrical Lorentzian form. The frequencies of the peaks of the lines were measured. These measurements can be reproduced to within about ±0.05 MHz. The frequencies of the peaks should in most cases be close to the frequencies of transitions not perturbed by nuclear quadrupole interaction. The frequency measurements made by this Stark spectrometer are therefore estimated to have an uncertainty of approximately ±0.15 MHz.

MP2/6-311++G** rotational constants and dipole moment components were also calculated for the *E* isomer. No transitions attributable to this isomer were identified in the Stark spectrum. It is concluded that this form cannot be present in high concentrations. This is in accord with previous findings.[1]

Fourier Transform MW Spectroscopy. The resolution and sensitivity of this supersonic molecular-jet technique is much higher than in the Stark experiment described above. The rotational temperature is much lower in the supersonic expansion (1−2 K), and this allows only ground-state transitions involving low values of the principal quantum number *J* and of the pseudo quantum number K_a to be observed.

The preliminary spectroscopic constants obtained in the Stark experiment were used to predict the frequencies of additional transitions. Weak *b*-type lines could be assigned using this technique. *c*-type lines were searched for, but none were identified.

It is found below that the equilibrium conformation is nonplanar. Tunneling between two equivalent forms should lead to a large splitting for the *c*-type transitions and much smaller splittings for the *a*- and the *b*-type lines. There is no indication of such splittings in the *a*- and *b*-type lines observed in this experiment, which is characterized by its extreme resolution.

A total of six a-type and seven *b*-type lines were observed for the parent molecule and assigned to $J = 0-4$, $K_a = 0-2$ transitions.

To maximize the signal-to-noise ratio, the molecules were polarized with an optimal microwave power of 0.1 and 2.5 mW for the *a*- and *b*-type transitions, respectively. This clearly indicates that the dipole moment components $\mu_a \gg \mu_b$, as predicted in the MP2 calculations and indeed found experimentally (see below).

A complex hyperfine structure caused by the presence of the two nitrogen atoms was seen for each of these transitions. One example is the fully resolved hyperfine structure of the $J_{K_a}K_c = 1_{11} \leftarrow 0_{00}$ *b*-type transition, which is shown in Figure 2.

The hyperfine structure was described with the two nuclear quadrupole interaction $\hat{H}_Q$ terms associated with *n*, the nitrogen nuclei of the cyano and amino groups, respectively, and written as[35]

$$\hat{H}_Q^{(n)} = \frac{1}{6}\sum_{ij}\hat{Q}_{ij}^{(n)}\hat{V}_{ij}^{(n)} \quad (3)$$

Equation 3 describes the interaction between the nuclear electric quadrupole moment $Q^{(n)}$ and the molecular electric field gradient $V^{(n)}$ for the nucleus *n*. The nuclear quadrupole coupling constants, $\chi^{(n)}_{\alpha\beta}$, are the elements of the quadrupole coupling tensor given by

$$\chi_{\alpha\beta}^{(n)} = eQ^{(n)}\frac{\partial^2 V^{(n)}}{\partial\alpha\,\partial\beta} \quad (4)$$

α and β refer to the coordinates *a*, *b*, and *c* of the principal inertial axis system, and *e* denotes the elementary charge. The angular momenta associated with the nitrogen nuclear spins were first coupled together, and the resulting momentum $\hat{I}$ was next added to the rotational angular momentum $\hat{J}$ to obtain the total angular momentum $\hat{F}$. The observed lines satisfy the selection rules $\Delta F = 0, \pm 1$ (*F* is the quantum number associated with the operator $\hat{F}^2$).

The 13 lines split by nuclear quadrupole coupling were first fitted to a Hamiltonian, which included only the diagonal elements of the quadrupole coupling constants of each nitrogen nucleus in addition to the rigid rotor (eq 1) and quartic centrifugal distortion parts (eq 2). The least-squares fit was performed with the program SPFIT by Pickett.[36] χ_{aa} and χ_{cc} of

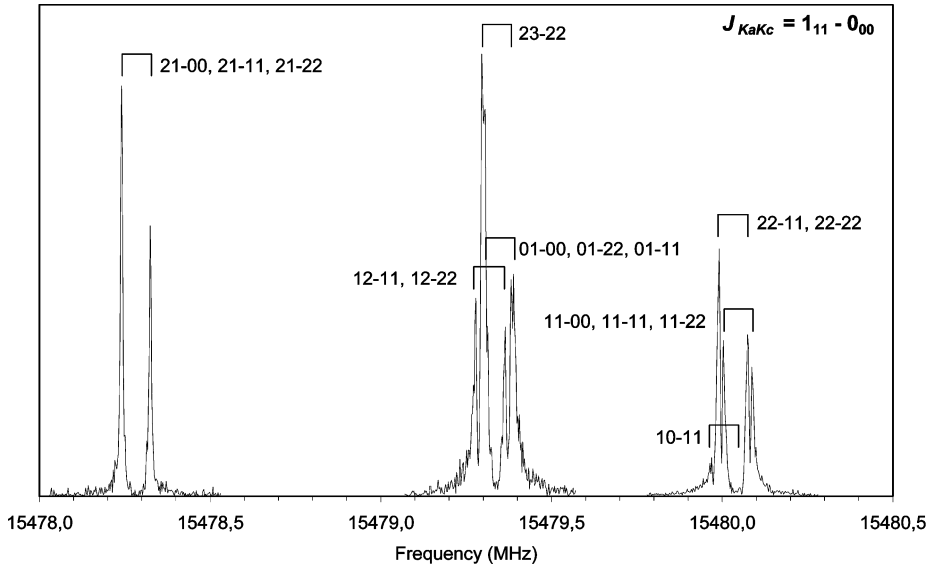

Figure 2. Composite microwave Fourier transform spectrum of the $1_{11} \leftarrow 0_{00}$ rotational transition of *Z*-3-amino-2-propenenitrile. The hyperfine structure associated with the two nitrogen nuclei is shown in detail. The lines are assigned with the *I*, *F* quantum numbers.

TABLE 1: Spectroscopic Constants[a] of the Ground and Vibrationally Excited States of *Z*-3-Amino-2-propenenitrile

state	ground	first excited out-of-plane	first excited in-plane	second excited in-plane
A (MHz)	12583.056(35)	12577.65(20)	12641.95(25)	12700.34(35)
B (MHz)	3766.1252(31)	3752.7271(63)	3771.0753(81)	3775.015(12)
C (MHz)	2896.3784(28)	2891.4408(62)	2895.3996(74)	2894.252(13)
Δ_J (kHz)	4.416(17)	4.339(12)	4.325(16)	4.261(21)
Δ_{JK} (kHz)	-31.068(98)	−30.210(26)	−30.499(36)	−29.041(45)
Δ_K (kHz)	46(35)	45.5[f]	45.5[f]	45.5[f]
δ_J (kHz)	1.4487(52)	1.372(14)	1.420(18)	1.375(28)
δ_K (kHz)	6.4(14)	6.42[f]	6.42[f]	6.42[f]
Δ[b]	0.1324(4)	-0.0660(11)	0.5546(14)	0.9475(22)
rms[c]	2.22[e]	0.094[g]	0.111[g]	0.125[g]
no.[d]	113	86	77	59

[a] *A*, reduction; I^r, representation.[31] Uncertainties represent one standard deviation. [b] $\Delta = I_c - I_a - I_b$. I_a, I_b, and I_c are the principal-axes moments of inertia. Conversion factor: $505\,379.05 \times 10^{-20}$ MHz u m^2. [c] Root-mean-square deviation. [d] Number of transitions. [e] Root-mean-square deviation of weighted fit. [f] Fixed. [g] Root-mean-square deviation (MHz) of fit with unit weights.

the two nuclei were varied in the least-squares fit. χ_{bb} was calculated from the relation $\chi_{aa} + \chi_{bb} + \chi_{cc} = 0$.

These 13 microwave lines were now "corrected" for quadrupole interactions. A weighted least-squares fit using ROTFIT[34] was then performed. The inverse squares of the estimated standard deviations of the measured frequencies were employed in a diagonal weight matrix. The frequencies corrected for quadrupole interaction of the transitions observed with the Fourier transform spectrometer were all assigned a standard deviation of 3 kHz, whereas the transitions observed using the Stark spectrometer were assigned a standard deviation of 50 kHz. Watson's Hamiltonian (*A* reduction I^r representation),[31] including quartic centrifugal distortion constants (eqs 1 and 2) were employed in a least-squares fit of all observed transitions. The resulting spectroscopic constants are listed in Table 1, and the spectrum is shown in Table 1S in the Supporting Information.

Comparison of the experimental rotational constants in this table with their MP2/6-311++G** counterparts given in the previous paragraph shows that the agreement is better than 2%, as expected. It is seen (Table 1) that three of the quartic centrifugal distortion constants (Δ_J, Δ_{JK}, and δ_J) are accurately determined, while Δ_K and δ_K are rather inaccurate. The experimental values of Δ_J, Δ_{JK}, and δ_J are in satisfactory agreement with the MP2 values given above.

Interestingly, the inertial defect Δ defined by $\Delta = I_c - I_a - I_b$, where I_a, I_b, and I_c are the principal moments of inertia is $\Delta = 0.1324(4) \times 10^{-20}$ u m^2 (Table 1). Δ is zero for a completely rigid and planar molecule. This relatively small deviation from zero is taken as an indication that the molecule is planar, or nearly planar[37] (see discussion below).

The final values of the quadrupole coupling constants were now determined. The values of the rotational and centrifugal distortion constants shown in Table 1 were kept fixed in the least-squares fit employing the SPFIT program.[36] The fit is shown in Table 2S in the Supporting Information. The results were $\chi_{aa} = -1.4917(21)$ and $\chi_{cc} = 1.5644(24)$ MHz for the nitrogen atom of the cyano group and $\chi_{aa} = 1.7262(18)$ and $\chi_{cc} = -4.0591(17)$ MHz for the nitrogen atom of the amino group. These values are also listed in Table 2 together with the corresponding χ_{bb} values. In addition, this table contains the experimental and theoretical HF/VTZ quadrupole coupling constants for acrylonitrile and vinylamine together with the corresponding values of APN. A discussion of the nuclear quadrupole constants is found in the Theoretical Section.

Vibrationally Excited States. The ground-state spectrum was accompanied by spectra that were presumed to belong to vibrationally excited states. The spectra of three such states were assigned using Stark spectroscopy, as seen in Tables 3S−5S in the Supporting Information. A least-squares fit of these spectra, assuming unit weights for the transitions, yielded the spectroscopic constants displayed in Table 1. As the quartic constants Δ_K and δ_K are rather poorly determined, they were held fixed in the fit at the values found for their counterparts of the ground vibrational state.

The vibrationally excited state that has the inertial defect $\Delta = -0.0660(11) \times 10^{-20}$ u m^2, is presumed to be the first excited state of the lowest out-of-plane vibration, because of the way in which Δ changes upon excitation of this mode.[37] The frequency of this fundamental vibration was determined to be 176(20) cm^{-1} by relative intensity measurements of MW transitions performed largely as described by Esbitt and Wilson.[38]

TABLE 2: Quadrupole Coupling Constants (MHz) for *Z*-3-Amino-2-propenenitrile, Vinyl Cyanide, and Vinylamine

	experimental			ab initio[a]						
	χ_{aa}	χ_{bb}	χ_{cc}	χ_{aa}	χ_{bb}	χ_{cc}	χ_{xx}	χ_{yy}	χ_{zz}	η^b
APN(CN)	−1.4917	−0.0727	1.5644	−1.21	0.064	1.145	−3.66	2.52	1.14	−0.377
vinyl cyanide	−3.7891	1.6861	2.1030	−3.44	1.620	1.816	−3.89	2.07	1.82	−0.065
APN(NH_2)	1.7262	2.3329	−4.0591	1.56	1.972	−3.53	1.58	2.06	−3.64	0.132
vinylamine	2.0722	2.0751	−4.1473	1.64	1.873	−3.51	2.12	1.80	−3.92	−0.082

[a] HF/VTZ level. [b] Asymmetry parameter for quadrupole coupling defined by $\eta = (\chi_{aa} - \chi_{bb})/\chi_{cc}$.

TABLE 3: Spectroscopic Constants[a] Isotopologues of *Z*-3-Amino-2-propenenitrile

species:	DHNCH=CHCN[e]	DHNCH=CHCN[g]	$H_2NCH{=}CDCN$	$H_2NCD{=}CHCN$	$H_2{}^{15}NCH{=}CHCN$	$H_2NCH{=}CHC^{15}N$	$H_2NCH{=}{}^{13}CHCN$	$H_2NCH{=}CH^{13}CN$
A (MHz)	11894.99(20)	12157.25(24)	11367.33(44)	12241.57(40)	12352.11(27)	12489.74(38)	*h*	*h*
B (MHz)	3753.381(13)	3607.428(13)	3763.719(26)	3640.609(17)	3704.155(14)	3656.845(16)	3773.787(4)	3731.693(4)
C (MHz)	2851.314(13)	2780.622(12)	2825.378(21)	2804.133(16)	2847.459(14)	2826.514(14)	2872.039(3)	2875.130(3)
Δ_J (kHz)	4.539(18)	4.202(17)	4.178(70)	3.6560(40)	4.421(30)	4.196(38)	4.42[f]	4.42[f]
Δ_{JK} (kHz)	-27.667(28)	−32.192(28)	−28.43(10)	−24.020(83)	−31.224(55)	−29.664(76)	−31.07[f]	−31.07[f]
Δ_K (kHz)	45.5[f]	45.5[f]	45.5[f]	45.5[f]	45.5[f]	45.5[f]	45.5[f]	45.5[f]
δ_J (kHz)	1.468(28)	1.372(22)	1.427(69)	1.120(48)	1.395(51)	1.387(47)	1.449[f]	1.449[f]
δ_K (kHz)	6.42[f]	6.42[f]	6.42[f]	6.42[f]	6.42[f]	6.42[f]	6.42[f]	6.42[f]
Δ^b	0.1112(19)	0.0862(19)	0.1359(35)	0.1255(27)	0.1341(20)	0.1350(24)	*h*	*h*
rms[c]	0.134	0.138	0.180	0.152	0.100	0.129	0.019	0.013
no.[d]	72	72	38	48	48	48	3	3

[a] *A*, reduction I^rrepresentation.[31] Uncertainties represent one standard deviation. [b] Inertial defect. Same units as in Table 1. [c] Root-mean-square deviation. [d] Number of transitions. [e] D−N−C=C in the synperiplanar configuration. [f] Fixed. [g] D−N−C=C in the antiperiplanar configuration. [h] Not determined.

Two successively excited states of the lowest in-plane bending vibration were also assigned, as shown in Table 1. This assignment is in accord with the fact that Δ becomes larger and positive upon excitation.[37] Relative intensity measurements[38] yielded a value of 152(20) cm^{-1} for this fundamental vibrational mode.

The harmonic vibrational frequencies have been calculated at various theoretical levels below. The results were 140 and 208 cm^{-1} (B3LYP/VTZ), 42 and 140 cm^{-1} (B3LYP/AVTZ), 136 and 267 cm^{-1} (MP2/6-311++G**), and 132 and 272 cm^{-1} (MP2/VTZ). These uncorrected values of the vibrational frequencies are therefore seen to vary considerably with the method used to derive them. The best agreement is found in the B3LYP/VTZ calculations (140 and 208 cm^{-1}) compared with the experimental values (152(20) and 176(20) cm^{-1}).

Assignments of Isotopologues. The changes of the MP2 rotational constants caused by isotopic substitution were added to the experimental rotational constants. The resulting rotational constants were used to predict the MW spectrum of the isotopologues. In this manner, the spectra of the isotopically enriched species (**3**, **5**−**8**) were found close to the predicted frequencies using Stark spectroscopy and readily assigned. The spectra of these species are found in Tables 6S−11S in the Supporting Information. The spectroscopic constants derived from them using unit weights in the least-squares fits are shown in Table 3.

The Stark spectra are fairly crowded and comparatively weak and could therefore not be employed to assign ^{13}C isotopologues in natural abundance. By use of the more sensitive Fourier transform spectroscopy, the spectra of two ^{13}C isotopologues were detected in their natural abundance (1.1%) after a careful search. They are associated with the ^{13}C isotopologues of the C2 and C3 atoms (Figure 1). Only three weak *a*-type rotational lines were detected for each species. Unfortunately, the spectrum associated with the ^{13}C isotopologue of the C1 atom could not be assigned because the signal-to-noise ratio was insufficient.

The spectra of the ^{13}C species are found in Tables 12S and 13S in the Supporting Information. Only the *B* and *C* rotational constants of each species could be determined from these spectra. The centrifugal distortion constants were fixed at the values of the parent species. The *B* and *C* rotational constants obtained in this manner are listed in Table 3.

TABLE 4: Second Order Stark Coefficients[a] and Dipole Moment of *Z*-3-Amino-2-propenenitrile

		stark coefficients $\Delta E^{-2}/(10^{-6}$ MHz $V^{-2})$ cm^2	
transition	$\lvert M\rvert$	obsd	calcd
$4_{1,4} \leftarrow 3_{1,3}$	0	−5.70(30)	−5.84
	1	3.90(20)	3.64
$4_{0,4} \leftarrow 3_{0,3}$	1	−5.30(20)	−5.31
$4_{1,3} \leftarrow 3_{1,2}$	0	−2.40(10)	−2.37
	1	−6.30(30)	−6.71
	2	−19.9(8)	−19.7
$5_{1,5} \leftarrow 4_{1,4}$	1	−2.00(10)	−1.99
$5_{0,5} \leftarrow 4_{0,4}$	1	−3.50(20)	−3.49

Dipole Moment

$\mu_a = 16.45(12)$, $\mu_b = 2.86(6)$, $\mu_c = 0$,[b] and $\mu_{tot.} = 16.70(12) \times 10^{-30}$ C m

[a] Uncertainties represent one standard deviation. 1 D = 3.33564×10^{-30} C m. [b] Preset at this value in the least-squares fit.

Dipole Moment. The dipole moment was determined in a least-squares fit using the second-order Stark coefficient shown in Table 4. The weight of each Stark coefficient was taken to be the inverse square of its standard deviation, which is also shown in the same table. The cell was calibrated using OCS, whose dipole moment was taken to be $2.3857(68) \times 10^{-30}$ C m.[39] The theoretical values of the second-order Stark coefficients were calculated as described by Golden and Wilson,[40] employing the computer program MB04.[41]

The dipole moment along the *c*-principal inertial axis, μ_c, should be exactly zero if APN were completely planar. A nonplanar molecule should have a nonzero μ_c, whose size should increase with increasing deviation from planarity. Care was therefore exercised to find Stark coefficients that are sensitive to this dipole moment component. Some of the Stark coefficients used in this fit depend strongly on μ_c.

All three principal-axis dipole moment components were initially varied in the fit. However, a small but negative value of $\mu_c^2 = -0.004 \times (10^{-30}$ C m$)^2$ with a comparatively large

TABLE 5: Cartesian Coordinates for *Z*-3-Amino-2-propenenitrile (pm)

	MP2/VQZ			experimental[a]		
	a	b	c	a_s	b_s	c_s
N_{amino}	149.8	−88.7	−3.5	150.58(10)	-88.51(17)	−3.0(49)[b]
C3	125.4	45.3	1.1	112.3(15)	17.0(10)	1.0(53)
C2	2.8	102.0	−0.1	8.0(22)[b]	101.9(16)	−3.0(14)
C1	−112.3	18.7	−0.1	−102.3[c]		
N_{cyano}	−200.7	−56.6	0.4	−201.73(7)	−56.55(27)	3.7(40)[b]
H_a	240.3	−122.4	23.2	241.70(12)	−121.73(25)	15.9(19)
H_s	72.6	−152.0	9.9	66.16(45)	−153.06(20)	10.6(28)
H(C3)	213.1	108.3	1.8	214.63(14)	108.71(28)	6.1(50)
H(C2)	−8.4	209.1	−1.5	−29.0(10)	208.27(14)	−4.4(68)[b]

[a] From Kraitchman equations, the uncertainties are calculated from Costain's rule: $\sigma(x) = 0.15/|x|$; for the H coordinates, this value is multiplied by 2. [b] Imaginary coordinate. [c] From first moment equation.

standard deviation of $0.050 \times (10^{-30}$ C m$)^2$ was found. The fit thus resulted in a small but imaginary μ_c with a relatively large uncertainty.

It is not possible to conclude from this result whether the molecule is completely planar or not. However, it can be stated that any deviation from planarity would not be large. In the final fit, which is shown in Table 4, μ_c has arbitrarily been fixed at zero. This has very little influence on the values of $\mu_a = 16.46(11) \times 10^{-30}$ C m [4.93(4) D] and $\mu_b = 2.86(6) \times 10^{-30}$ C m [0.862(2) D], which were obtained in this manner.

The dipole moment has been calculated below at various levels of theory, with MP2/VQZ as the highest level. The results of the MP2/VQZ calculations were $\mu_a = 17.9$, $\mu_b = 3.26$, and $\mu_c = 1.96 \times 10^{-30}$ C m. Two conclusions can be drawn: The theoretical dipole moment components are typically higher than their experimental counterparts. The MP2/VQZ value of μ_c is calculated to be comparatively small, since a nonplanar equilibrium conformation is predicted (see below).

Attempts To Calculate the Structure from the Experimental Rotational Constants. One aim of this work has been to derive an accurate molecular structure of APN. According to Costain,[42] the rotational constants of the ground vibrational state of the parent molecule and of isotopologues can be used to calculate a set of Cartesian coordinates, so-called substitution (r_s) coordinates, for atoms that have been substituted by an isotope. Kraitchman's equations[43] are employed for this purpose. The coordinates obtained in this manner could be obtained for all atoms of APN but C1. The coordinates are listed in Table 5 together with the MP2/VQZ values. Four of the small Kraitchman coordinates were imaginary (Table 5). Kraitchman's equations yield the absolute values of the coordinates. The signs assigned to the r_s coordinates in Table 5 have been chosen to make them consistent with the signs obtained in the MP2/VQZ calculations.

The spectrum of $H_2NCH{=}CH^{13}CN$ could not be assigned. It was therefore not possible to calculate Kraitchman's coordinates for this atom. The *a*-coordinate of C1 appearing in Table 5 was instead calculated using the first moment equation.[42] The *b*- and *c*-coordinates of this atom can be derived in the same manner, but they have not been listed in this table because they are small and have large uncertainties.

Costain[44] and van Eijck[45] have discussed the accuracy of substitution coordinates. The uncertainties of the r_s coordinates of the carbon and nitrogen atoms shown in Table 8 have been calculated using Costain's rule,[44] $\sigma(x) = (0.15$ pm$^2)/|x|$, where $\sigma(x)$ is the uncertainty and x is the Kraitchman coordinate. The uncertainties of the hydrogen atoms have been calculated using $\sigma(x) = (0.30$ pm$^2)/|x|$.

The existence of a near-symmetry plane in APN results in a series of small *c*-coordinates with relatively large uncertainties (Table 5). There is also a small *a*- (C2 atom) and a small *b*-coordinate (C1 atom).

There is a satisfactory agreement between the r_s and the MP2/VQZ coordinates shown in Table 5. However, the delicate question of whether the compound is planar or not cannot be settled using the r_s coordinates of this table, because all *c*-, one *a*-, and one *b*-coordinate have comparatively large uncertainties. It was discovered during the course of this work that the ab initio calculations presented in the next section were able to yield an equilibrium structure that is superior to the r_s structure that can be calculated from the experimental rotational constants obtained in this study. These calculations were also able to resolve the planarity problem. A full r_s structure is therefore not presented here. The reader is instead referred to the ab initio structure presented in the next section.

Theoretical Section

Strategy To Derive the Equilibrium Structure. A major objective of this study has been to derive an accurate equilibrium structure of APN using quantum chemical methods. Ab initio calculations are in principle limited in scope and will consequently not predict the exact equilibrium structure. However, using small model molecules, it is now possible to extrapolate to their very accurate equilibrium structures.[46−48] The differences between the bond lengths obtained in high-level ab initio calculations and their equilibrium counterparts will be called offsets. It is a reasonable assumption that offsets obtained for a small molecule can be transferred to a larger, closely related, molecule. This is the strategy that will be used to obtain the equilibrium structure of APN.

One way of obtaining useful offsets for APN would be to transfer them from $CH_2{=}CHCN$ and vinylamine, $CH_2{=}CHNH_2$, since the title compound may be considered either as an amino derivative of vinyl cyanide or as a cyano derivative of vinylamine. The procedure has therefore been to first calculate accurate equilibrium structures both for vinyl cyanide and for vinylamine, because these two compounds are more easily amenable to high-level ab initio calculations than APN, since they consist of fewer first-row atoms than $H_2NCH{=}CHCN$. The offsets obtained in these calculations will then be transferred to APN.

Methods of Calculations. Most of the correlated-level ab initio electronic structure computations conducted during the course of this study of the equilibrium structure have been carried out at two levels: second-order Møller−Plesset perturbation theory (MP2)[30] and coupled cluster (CC) theory with single and double excitation[49] augmented by a perturbational estimate of the effects of connected triple excitations [CCSD(T)].[50] The Kohn−Sham density functional theory[51] using

TABLE 6: Ab Initio Geometries (Distances, pm; Angles, deg) of Vinyl Cyanide[a]

	MP2					CCSD(T)						
	VTZ	VQZ	AVQ Z	wCVQZ	wCVQZ(ae)	VDZ	VTZ	VQZ	VZ$^{\infty,b}$	r_e^c	old r_e^d	$r_m^{\rho\,e}$
r(C=C)	133.74	133.49	133.50	133.45	133.13	135.62	134.13	133.84	133.76	133.52	133.7	133.3(3)
r(C−C)	142.91	142.73	142.74	142.7	142.37	145.22	143.84	143.65	143.61	143.32	143.2	142.9(3)
r(CN)	117.27	116.97	117.01	116.92	116.63	117.96	116.47	116.13	116.02	115.84	115.7	115.7(3)
r(C−H_t)	107.92	107.83	107.83	107.82	107.67	109.66	108.16	108.08	108.07	107.93	108.0	108.8(1)
r(C−H_c)	107.98	107.89	107.89	107.88	107.73	109.70	108.21	108.13	108.12	107.98	108.1	109.7(2)
r(C−H_g)	108.06	107.99	107.99	107.99	107.84	109.72	108.23	108.17	108.17	108.02	108.2	109.3(4)
∠(CCC)	122.191	122.088	122.04 4	122.073	122.105	122.051	122.126	122.040	122.040	122.072	122.1	122.5(5)
∠(CCN)	179.117	179.184	180.00 0	180.000	180.000	179.382	179.067	179.125	179.125	179.125	179.2	180.7(9)
∠(CCH_t)	120.311	120.296	120.29 5	120.298	120.321	120.378	120.406	120.385	120.385	120.408	120.3	120.3(fixed)
∠(CCH_c)	121.220	121.189	121.18 5	121.189	121.196	121.440	121.375	121.345	121.319	121.352	121.5	120.2(1)
∠(CCH_g)	121.265	121.362	121.41 7	121.371	121.338	121.657	121.647	121.730	121.730	121.697	121.5	121.7(2)

[a] Frozen core approximation unless otherwise stated; ae = all electrons correlated. g = geminal, c = cis to CN, and t = trans to CN. [b] Exponential extrapolation to infinite basis set. [c] CCSD(T)/VQZ + MP2(ae)/wCVQZ − MP2(fc)/wCVQZ. [d] Reference 63. [e] Reference 64.

Becke's three-parameter hybrid exchange functional,[52] and the Lee−Yang−Parr correlation functional,[18] together denoted as B3LYP, was also used in this study. The G3 method[53] was employed in the calculations of reaction paths.

The correlation-consistent polarized *n*-tuple ζ basis sets cc-pV*n*Z[54] with $n \in \{D, T, Q, 5\}$ were employed extensively in this study. In this paper, these basis sets are abbreviated as V*n*Z. For several CCSD(T) calculations, a mixed basis set denoted as V(T,D)Z was utilized. It is composed of VTZ on all non-hydrogen atoms and VDZ on H. Such a basis set reduces the computation time significantly and has been shown to be able to predict the structure of the heavy atom skeleton accurately.[55] To account for the electronegative character of the N atom, the augmented V*n*Z (aug-cc-pV*n*Z, AV*n*Z in short) basis sets[56] were also employed, particularly at the MP2 level. The combination of an AVQZ basis on all non-hydrogen atoms and of VQZ on H is denoted hereafter as A′VQZ.

To estimate the core−core and core−valence correlation effects on equilibrium geometries,[57] the correlation-consistent polarized weighted core−valence *n*-tuple ζ (cc-pwCV*n*Z)[58,59] basis sets were employed. As for the effect of inclusion of diffuse functions in the basis set, it is sufficient to use the MP2 method to estimate this correction.[48] The frozen core approximation (hereafter denoted as fc), i.e., keeping the 1s orbitals of C, N, and O doubly occupied during correlated-level calculations, was used extensively.

The CCSD(T) calculations were performed with the MOLPRO[60−62] electronic structure program packages, while most other calculations utilized the GAUSSIAN 03 program.[32]

Equilibrium Structure of Vinyl Cyanide. The structure of vinyl cyanide has been the subject of previous investigations. An ab initio structure was calculated at the MP2 level, and a near-equilibrium structure was estimated using corrections derived empirically.[63] More recently, the pure rotational spectra of 13 isotopologues of vinyl cyanide have been measured, and the derived rotational constants have been used to evaluate the molecular geometry using various methods.[64] It was found that the empirical substitution (r_s)[42] and r_m^{ρ} structures[65] are in general in excellent agreement with the ab initio values.

It has been established that vinyl cyanide is planar; its geometry was therefore optimized with the constraint of C_s symmetry. The details of the computed geometries are given in Table 6. The coupled cluster T_1 diagnostic[66] at the CCSD(T)/VQZ of theory is 0.014, indicating that the CCSD(T) results should be reliable. Improvement of the basis set from VTZ to VQZ leads to negligible changes for the bond angles as well as for the C−H bond lengths. For the CC and CN bond lengths, there is a decrease of about 0.2−0.3 pm, indicating that convergence is nearly achieved but that these ab initio bond lengths may be slightly too long. Addition of diffuse functions on all heavy atoms leads to negligible changes in the bond lengths and angles.

To estimate the inner-shell correlation, the MP2 method was used. It leads to the expected shortening of the bonds: C−H (0.15 pm), CC (0.32 pm), and CN (0.29 pm). The effect on the angles is negligible. The most reliable ab initio structure is obtained by correcting the CCSD(T)/VQZ values for the effects of inner-shell correlation. It is given in Table 6. If an exponential extrapolation to infinite basis size is tried, it has a significant effect on the C≡N bond length only, which is shortened by 0.1 pm.

The r_e structure (Table 6) is in excellent agreement with the previous one,[63] which is also given in the same table. Comparison of this structure with the MP2/VQZ results shows that there is a good agreement for the bond angles and the C=C bond length, but the MP2 C−C, C≡N, and C−H bond lengths are too short by 0.6, 1.1, and about 0.1 pm, respectively. These offsets will be used in the derivation of the equilibrium structure of APN below, for which MP2/VQZ calculations were performed.

The equilibrium structures of two compounds related to vinyl cyanide, namely, *Z*-pent-2-en-4-ynenitrile (N≡C−CH=CH−C≡CH) and maleonitrile (N≡C−CH=CH−C≡N) have been reported.[67] The r_e lengths of the C≡N bonds in these two molecules are 115.7 and 115.8 pm, respectively, compared to 115.8 pm in vinyl cyanide (Table 6), whereas the C=C equilibrium bond lengths are 134.5 pm in *Z*-2-en-4-ynenitrile and 134.1 in maleonitrile, slightly longer than 133.5 pm in vinyl cyanide.

Equilibrium Structure of Vinylamine. Vinylamine is the simplest enamine and is thought to be a constituent of interstellar molecular clouds.[68] Although it is a short-lived transient species, which is difficult to generate, it has been studied by microwave,[22,24] infrared,[69] and ultraviolet[70] spectroscopies. The structure was first determined by microwave spectroscopy, and the molecule was found to be nonplanar.[21] The nonplanarity was confirmed by a combined semirigid bender analysis of vibrational satellite shifts in the microwave spectrum and infrared data.[70] The ab initio structure was also calculated in a number of investigations,[69] but the highest level of calculation was MP2/6-311G**, which is not always sufficient to obtain an accurate geometry.

The structure was first calculated at the MP2 level with the VTZ and VQZ basis sets and the CCSD/VTZ and CCSD(T)/V(T,D)Z levels. All these calculations indicate that the vinyl group $H_2C{=}CH$ is planar. Finally, the structure was calculated

TABLE 7: Ab Initio Geometries (Distances, pm; Angles, deg) of Vinylamine[a]

	MP2/VTZ	MP2/VQZ	MP2/wCVQZ	MP2(ae)/ wCVQZ	CCSD/VTZ	CCSD(T)/V(D,T)Z	CCSD(T)/VTZ plan	r_e[b]	r_s
C═C	133.79	133.56	133.52	133.21	133.48	134.05	134.11	133.57	133.5
C−H_{cis}	108.10	108.02	108.01	107.86	108.21	108.96	108.36	108.13	109.0
C−H_{trans}	107.70	107.62	107.61	107.45	107.81	108.57	107.95	107.71	109.0
C−N	139.33	138.95	138.91	138.54	139.94	140.19	140.21	139.46	139.7(40)
C−H_{gem}	108.25	108.17	108.16	108.01	108.27	109.04	108.42	108.19	109.0
N−H_{cis}	100.83	100.67	100.67	100.53	100.77	101.82	101.01	100.71	101.0
N−H_{trans}	100.66	100.49	100.49	100.35	100.64	101.70	100.87	100.56	101.0
∠CCH_{cis}	121.585	121.620	121.622	121.630	121.757	121.641	121.721	121.763	
∠CCH_{trans}	119.987	119.925	119.928	119.943	120.224	120.298	120.182	120.136	
∠HCH	118.417	118.445	118.441	118.418	118.009	118.051	118.097	118.103	118.0
∠CCN	126.131	126.040	126.035	126.066	126.149	125.974	126.019	125.959	125.2(20)
∠CCH_{gem}	119.944	120.005	120.001	119.959	120.073	120.196	120.127	120.146	
∠NCH	113.795	113.838	113.847	113.865	113.656	113.689	113.698	113.759	
∠CNH_{cis}	113.807	114.475	114.501	114.772	113.312	113.030	113.166	114.104	
∠CNH_{trans}	114.074	114.728	114.756	115.040	113.412	113.170	113.289	114.227	
∠HNH	110.985	111.549	111.580	111.849	110.364	110.182	110.327	111.160	114.0
∠H_cCCN	−4.023	−3.807	−3.799	−3.688	−3.881	−4.315	−4.824	−4.498	
∠H_cCCHg	−179.617	−179.616	−179.614	−179.621	−179.602	−179.726	180.000	180.000	
∠H_tCCN	174.728	175.045	175.058	175.193	174.922	174.508	175.176	175.629	
∠H_tCCH_g	−0.866	−0.764	−0.758	−0.740	−0.799	−0.903	0.000	0.000	
∠$CCNH_c$	18.875	18.368	18.366	18.089	19.152	18.958	20.293	19.510	
∠$CCNH_t$	147.619	149.208	149.305	150.000	145.987	145.095	146.844	149.127	
∠H_gCNH_c	−165.297	−165.599	−165.596	−165.764	−164.890	−165.372	−164.263	−164.734	
∠H_gCNH_t	−36.553	−34.760	−34.657	−33.853	−38.056	−39.236	−37.712	−35.116	

[a] Frozen core approximation unless otherwise stated; ae = all electrons correlated. [b] CCSD(T)/VTZ + MP2/VQZ − MP2/VTZ + MP2(ae)/wCVQZ − MP2(fc)/wCVQZ. ∠(CNH_s) + ∠(CNH_t) + ∠(HNH) = 339.5° (360° for a planar molecule)

TABLE 8: Ab Initio Geometries (Distances, pm; Angles, deg) of *Z*-3-Amino-2-propenenitrile[a]

	Z-3-amino-2-propenenitrile					
method:	B3LYP/VTZ	MP2/VTZ	MP2/VQZ	r_e[b]	vinyl cyanide MP2/VQZ	vinylamine MP2/VQZ
r(C3−N)	135.39	136.18	135.75	136.26		138.95
r(NH_t)	100.19	100.26	100.10	100.15		100.49
r(NH_s)	100.66	100.76	100.64	100.69		100.67
r(C2═C3)	135.31	135.27	135.09	135.11	133.49	133.56
r(C3−H)	108.21	108.11	108.03	108.06	107.83	108.17
r(C1−C2)	141.27	141.78	141.54	142.12	142.73	
r(C2−H)	107.80	107.60	107.53	107.63	107.99	107.62
r(C1−N)	115.66	117.51	117.22	116.09	116.97	
∠($C3NH_a$)	120.19	118.15	118.92			114.73
∠($C3NH_s$)	119.92	117.70	118.42			114.48
∠(HNH)	117.27	115.77	116.47			111.55
∠(C2C3N)	126.29	125.33	125.13			126.04
∠(NC3H)	114.80	115.29	115.38			113.84
∠(C2C3H)	118.90	119.33	119.45		120.30	120.01
∠(C1C2C3)	121.29	119.59	119.23		122.09	
∠(C3C2H)	120.00	120.66	120.82		121.36	119.93
∠(NC2H)	118.70	119.75	119.94			
∠(C2C1N)[d]	177.47	176.03	175.50		179.18	
∠(H_aNC3C2)	−168.94	−160.38	−163.11			−149.21
∠(H_aNC3H)	12.59	22.49	19.34			34.76
∠(H_sNC3C2)	−7.79	−13.47	−11.72			−18.37
∠(H_sNC3H)	173.74	169.40	170.73			165.60
∠(NC3C2C1)	1.97	3.43	2.95			
∠(NC3C2H)	−177.85	−176.19	−176.74			−175.05
∠(C1C2C3H)	−179.61	−179.55	−179.59			
∠(HC2C3H)	0.57	0.83	0.72			
∑[c]	357.4	351.6	353.8			340.8

[a] See Figure 1 for atom numbering. [b] Estimated from the MP2/VQZ structure using offsets derived from acrylonitrile and vinylamine. [c] ∠(CNH_s) + ∠(CNH_a) + ∠(HNH) (360° for a planar molecule). [d] N atom approaches the amino group.

at the CCSD(T)/VTZ level assuming planarity of the vinyl group. Then, the CCSD(T)/VQZ values were estimated using the following approximate formula CCSD(T)/VQZ ≈ CCSD(T)/VTZ + MP2/VQZ − MP2/VTZ. There is indeed large, documented evidence that this formula is a good approximation,[46−48] and this was again verified here in the particular case of vinyl cyanide (see Table 6).

As in the previous case of vinyl cyanide, the equilibrium structure is obtained by correcting the CCSD(T)/VQZ values for the effects of inner-shell correlation calculated at the MP2/wCVQZ level; see Table 7. Vinylamine is confirmed to be nonplanar, and the N−H bond lengths are characteristic of a nonplanar NH_2 group.[55] It may also be noted that the *gem* C−H bond length is shorter than the other two, which are almost identical.

Comparison of this structure with the MP2/VQZ results shows that there is good agreement for the bond angles and the C═C

and N−H bond lengths, but the MP2 C−N bond length is too short by 0.5 pm, which is taken to be the offset for this distance.

Equilibrium Structure of APN. The structure has been calculated at the MP2/VQZ level of theory (Table 8). The use of the MP2 method significantly reduces the complexity of the determination of the electron correlation energy, whereas it gives structural parameters with an accuracy just slightly inferior to that of the CCSD(T) method, at least for molecules including only first-row atoms.[29,71] This was confirmed above for vinyl cyanide and vinylamine (Tables 6 and 7).

MP2 calculations may give reliable equilibrium bond angles, with an accuracy of a few tenths of a degree.[46] On the other hand, the offset error, which is due to the finite size of the basis set, and to the partial consideration of electron correlation, remains in bond lengths. For example, for the C−H bond length, the offset is nearly independent of the environment and may thus be easily estimated.[63] This remains true for the N−H bond length of different molecules, with exceptions, such as HNO.[47]

The structure of APN is shown in Table 8 together with the structures of vinyl cyanide and vinylamine. An equilibrium structure of APN has been estimated using the offsets determined for the bond lengths found for vinyl cyanide and vinylamine, as described in the preceding two paragraphs. The offsets of bond angles are assumed to be zero. The bond lengths and bond angles of the equilibrium structure are estimated to be accurate to within ±0.2 pm and ±0.2°, respectively. The accuracy of the dihedral angles is more difficult to estimate exactly and could be as large as a few degrees.

It is concluded that the equilibrium structure of APN is definitely nonplanar, since the sum of the $\angle CNH_s + \angle CNH_a + \angle HNH$ angles is significantly less than 360° (Table 8). This sum is even less in vinylamine, which is therefore more nonplanar than APN. One consequence of this difference is that the $\angle(HNH)$ and $\angle(C_3NH)$ angles are larger in APN than in vinylamine. Interestingly, the H_a of the amino group is more out of plane than the H_s atom.

The rotational constants of APN calculated from the r_e structure in Table 8 are $A = 12514.24$, $B = 3803.94$, and $C = 2920.01$ MHz. They agree to within better than 1% with the r_0 rotational constants (Table 1), which are 12583.056(35), 3766.1252(31), and 2896.3784(28) MHz, respectively. This difference was expected since the equilibrium (r_e) and effective (r_0) rotational constants are defined differently.

Quadrupole Coupling Constants. If the molecule has a symmetry plane and if the C≡N bond lies in this symmetry plane, the quadrupole coupling constant χ_{cc} (c being the principal axis perpendicular to the plane) is expected to be close to 2 MHz as, for instance, in vinyl cyanide[64] where $\chi_{cc} = 2.10$ MHz, or its methyl derivatives.[72] Likewise, if the NH_2 group lies in the symmetry plane, χ_{cc} is expected to be negative and larger than −4 MHz.[55]

For these reasons, it is interesting to compare the quadrupole coupling constants of APN with those of vinyl cyanide and vinylamine. However, if the molecule is not planar (which seems to be the case for APN), this comparison is made difficult by the fact that these constants are given for the principal inertial axis system. To circumvent this difficulty, we have calculated the quadrupole coupling tensors of these molecules at the HF/VTZ level of theory. This level was chosen because, in a previous work on amides,[55] we found that it gives satisfactory results. The results are given in Table 2. For the cyano group, the χ_{zz} principal component is much larger in vinyl cyanide than in APN and the asymmetry much lower. It has also to be noted that, in APN, the angle $\angle(CC{\equiv}N)$ is significantly different from 180° (Table 8), whereas it is nearly linear in vinyl cyanide. Likewise, for the amino group, the χ_{zz} principal component is also significantly larger in vinylamine. Thus, it may be concluded that the bonding is different in APN compared to both vinyl cyanide and vinylamine.

Planarity. The principal inertial axis dipole moment components, the substitution coordinates, and the inertial defect are experimental parameters often used to decide whether a compound is planar or not. A small, positive value for the inertial defect, as observed for APN, is often interpreted as evidence that a molecule is planar, or nearly planar.[35] The small, imaginary experimental value of μ_c (see above) and the fact that no c-type transitions were assigned might also be an indication that APN is planar. However, a small degree of nonplanarity should lead to a small dipole moment along the c-axis. The MP2/VQZ calculations predict for example $\mu_c = 1.96 \times 10^{-30}$ C m [0.59 D]. It should be noted that the ab initio values of dipole moments tend to be too large, so 1.96×10^{-30} C m is presumably an upper limit of the dipole moment. Moreover, the dipole moment is *not* measured in the equilibrium conformation but in the effective ground-state conformation. This difference may obscure the physical significance of a small dipole moment component. It is interesting to note that the energy difference between the planar form and the minimum of the nonplanar form is indeed quite small. A value of only −423 J/mol (35.4 cm^{-1}) was obtained for this difference in the MP2/VQZ calculations. This indicates that the barrier is well below the zero-point level. The NH_2 group would therefore have equal amplitudes above and below the plane, and the vibrationally averaged c-component of the dipole moment should be zero. This could perhaps explain why μ_c is indistinguishable from zero and why no c-type lines were observed.

It was noted above the r_s coordinates (Table 5) cannot be used to decide whether the molecule is planar or not. However, the ground-state inertial defect of APN is as small as $0.1324(4) \times 10^{-20}$ u m^2 (Table 1). The equilibrium inertial defect calculated from the equilibrium structure in Table 7 is $\Delta_e = -0.167$ (same units), and the vibrational contribution calculated from the MP2/VTZ harmonic force field is $\Delta_v = +0.22$ ($+0.15 \times 10^{-20}$ u m^2 were found at the B3LYP/VTZ level of theory), giving $\Delta_0(\text{calc}) = +0.05 \times 10^{-20}$ u m^2, not widely different from the experimental value $(0.1324(4) \times 10^{-20}$ u $m^2)$. The vibrational contribution to the inertial defect is therefore of the same order of magnitude, but of opposite sign of Δ_e. It is concluded that even if the experimental ground-state inertial defect is quite small $(0.1324(4) \times 10^{-20}$ u m^2 in the present case), it is not necessarily in conflict with a slightly nonplanar structure. The present discussion once more shows how difficult it is to use ground-state observations to form conclusions about the equilibrium conformation of a compound, especially when an easily distortable group, such as the amino group, is involved.

Formation of APN via a Neutral−Neutral Reaction. It was noted above that *Z*- and *E*-3-amino-2-propenenitrile is formed in an approximately 1:1 mixture simply by mixing gaseous ammonia and cyanoacetylene at room temperature.[2,3] A mechanism suggested for this reaction is sketched in Figure 3. The relative enthalpy values (298.15 K, 1 atm) listed on this figure were calculated using the G3 method,[53] which is tailored to calculate energy differences accurately. The sum of the enthalpies of the reactants ammonia and cyanoacetylene were assigned a value of zero.

In the first step of this mechanism, a hydrogen-bonded complex ($H_3N{\cdots}H{-}C{\equiv}C{-}C{\equiv}N$) is formed between ammonia and cyanoacetylene, where the dots represent the hydrogen bond.

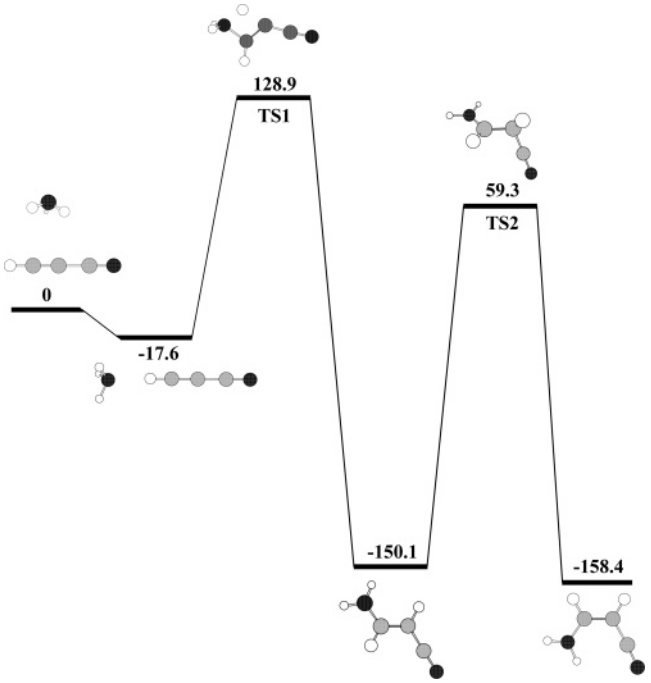

Figure 3. Reaction profile of the reaction between NH_3 and H−C≡C−C≡N forming *Z*- and *E*-3-amino-2-propenenitrile (H_2N−CH=CH−C≡N), as calculated using the G3 method. The numbers in the figure are enthalpy differences (298.15 K, 1 atm) in kilojoules per mole relative to the sum of the enthalpies of ammonia and cyanoacetylene, which has been assigned the value of zero.

The MW spectrum of this complex has been reported.[73] It is stabilized by $\Delta H = -18$ kJ/mol relative to the reactants ammonia and cyanoacetylene according to the G3 calculations. B3LYP/6-31G(d,p) calculations yield $\Delta E = -24$ kJ/mol for this energy difference, where ΔE is the energy of the hydrogen-bond formation corrected for zero-point vibrational effects, basis set superposition error, and relaxation correction.[74] MP2 calculations of the structure of this complex have been performed using Dunning's[54] correlation-consistent wave function of triple-ζ quality with polarized valence electrons, aug-cc-pVTZ. The complex is a symmetrical top with C_{3v} symmetry. The bond lengths were calculated to be r(N≡C1) = 117.5, r(C1−C2) = 137.2, r(C2≡C3) = 122.0, r(C3−H) = 107.7, and r(N−H) = 101.3 pm, whereas the NHN angle was 106.5°. The hydrogen bond length was r(H···N) = 213.7 pm. The *B* rotational constant calculated from this structure is 1102.62 MHz, compared to 1095.4628(11) MHz found experimentally for the ground vibrational state.[73]

This complex passes through a transition state (TS1) whose G3 enthalpy is 129 kJ/mol higher than the sum of the enthalpies ammonia and cyanoacetylene. MP2/aug-cc-pVTZ calculations of the structure and vibrational frequencies of TS1 have been performed. A model of the TS1 with atom numbering is shown in Figure 4 and its structure is given in Table 9. One imaginary vibrational frequency of -1469 cm^{-1} was calculated for this proper transition structure. This vibration is associated with the breaking of the H9−N5 bond and the formation of the H9−C2 bond.

It was shown[1] that a thermal interconversion path exists between the *Z*- and the *E*-forms. The transition structure associated with this transformation is denoted TS2 (Figure 3). The MP2/6-311+G(3df,2p) structure of TS2 has been reported elsewhere.[1] The G3 enthalpy of TS2 is 59 kJ/mol higher that that of the reactants (Figure 3). However, the enthalpy of TS2 is significantly lower than that of TS1 (129 kJ/mol). This implies

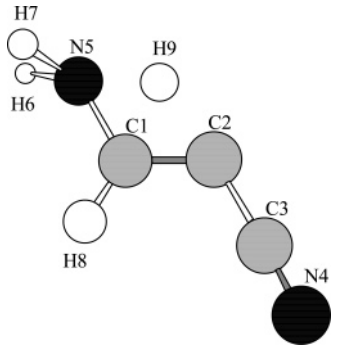

Figure 4. Model of TS1 with atom numbering.

that TS1 can be transformed to *both* the *E*- and the *Z*-forms, even if the *E*-configuration is about 8 kJ/mol less stable. This is in accord with the observation[2,3] that a 1:1 mixture of *E* and *Z* is formed at room temperature.

The temperature varies in the interstellar space, being typically a few kelvin in cold interstellar clouds. Spontaneous formation of APN can hardly occur in such clouds because of the high activation energy (about 129 kJ/mol). However, it is possible that this mechanism might produce APN in regions in space where the temperature is relatively high, on surfaces of interstellar grain, or in solution. Heating incidents might release APN from the grain to the gas phase.

Formation of APN via a Neutral-Cation Reaction. It is assumed that many of the compounds found in cold interstellar clouds have been formed spontaneously via a reaction between a cation and a neutral molecule.[75] These reactions occur because the activation energy is often low or nonexistent.

An alternative reaction path could in our case be that ammonia reacts with protonated cyanoacetylene (H−C≡C−C≡N−H$^+$) following a mechanism analogous to that outlined in the previous paragraph. The reaction profile based on G3 calculations is sketched in Figure 5. The energies shown in this figure are enthalpy differences (298.15 K, 1 atm).

The first step is the formation of a hydrogen-bonded complex, H_3N···H−C≡C−C≡N$^+$, stabilized by $\Delta H = -62$ kJ/mol relative to the enthalpies of the reactants. The first transition structure, TS3, has $\Delta H = 12$ kJ/mol compared to the combined enthalpies of ammonia and protonated cyanoacetylene. This represents a substantial reduction of the activation energy (from about 129 kJ/mol) of the neutral−neutral reaction, as expected. The transitions state for the $Z \rightarrow E$ interconversion (TS4) has $\Delta H = -172$ kJ/mol. Interestingly, the *E* isomer of the protonated 3-amino-2-propanenitrile (H_2NCH=CHCNH$^+$) is predicted to be favored by $\Delta H = 12$ kJ/mol (Figure 5) relative to the *Z*-form, which is the opposite of what is found for their counterparts in the neutral−neutral reaction. Neutral APN might then be formed in an electron recombination reaction.

APN might be formed by this mechanism in interstellar space at low temperatures since the activation energy is relatively low (+12 kJ/mol). However, a collision between protonated cyanoacetylene and ammonia might easily lead to the formation of cyanoacetylene and the ammonium cation instead, because of the high proton affinity of ammonia. The mechanism of Figure 5 is therefore considered to be of minor importance for the generation of interstellar APN.

Discussion

The bonding situation in APN is interesting. Comparison with vinylamine and vinyl cyanide is informative. The title compound is definitely flatter than vinylamine. The quadrupole coupling

TABLE 9: MP2/aug-cc-pVTZ Geometry of Transition Structure T1[a]

bond length (pm)		angle (deg)		dihedral angle (deg)	
$r(C_1-C_2)$	133.8	$\angle(C_1C_2C_3)$	124.2	$\angle(H_8C_1N_5H_9)$	180.0
$r(C_2-C_3)$	141.2	$\angle(C_2C_3N_4)$	175.0	$\angle(H_8C_1N_5H_6)$	−65.1
$r(C_3-N_4)$	117.8	$\angle(N_5C_1C_2)$	103.9	$\angle(C_1C_2N_5H_9)$	0.0
$r(C_1-N_5)$	148.2	$\angle(C_1N_5H_6)$	115.3	$\angle(H_6N_5C_1C_2)$	114.9
$r(N_5-H_6)$	101.8	$\angle(C_1N_5H_7)$	115.3	$\angle(H_8C_1C_2C_3)$	0.0
$r(N_5-H_7)$	101.8	$\angle(H_7N_5H_6)$	110.2	$\angle(N_5C_1C_2C_3)$	180.0
$r(C_1-H_8)$	108.3	$\angle(H_8C_1C_2)$	136.6	$\angle(H_8C_1N_5H_7)$	65.1
$r(C_2-H_9)$	157.0	$\angle(H_8C_1N_5)$	119.5	$\angle(H_7N_5C_1C_2)$	−114.9
$r(N_5-H_9)$	121.9	$\angle(C_1C_2H_9)$	72.4		
		$\angle(H_7N_5H_9)$	117.2		
		$\angle(C_1N_5H_9)$	78.8		
		$\angle(H_6N_5H_9)$	117.2		

[a] See text.

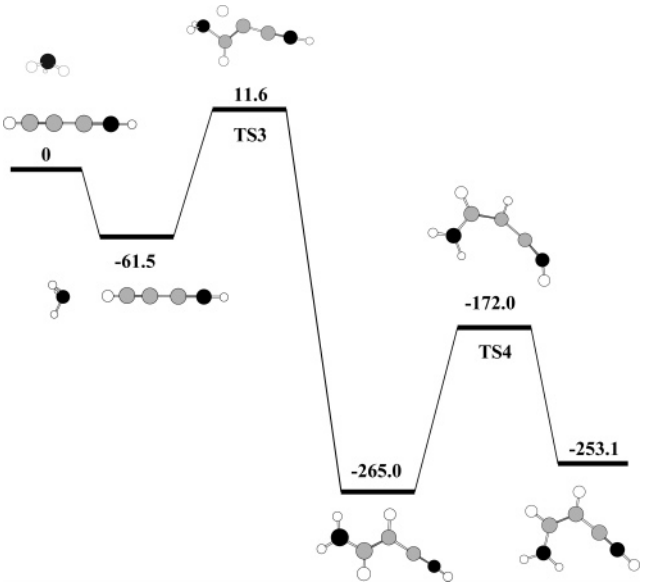

Figure 5. Reaction profile of the reaction between NH_3 and $H-C{\equiv}C-C{\equiv}N-H^+$ forming *Z*- and *E*-$H_2N-CH{=}CH-C{\equiv}N-H^+$, as calculated using the G3 method. The numbers indicated on this figure are enthalpy differences (298.15 K, 1atm) relative to the sum of the enthalpies of ammonia and protonated cyanoacetylene, which has been assigned the value of zero.

constants of the nitrogen atom of the cyano group is remarkably different in the two molecules, as noted above. Inspection of Table 8 reveals that the C2=C3 bond length is longer in APN than in both vinylamine and vinyl cyanide. It is also noted that the C1−C2 bond length is shorter in APN than in vinyl cyanide, whereas the C1≡N bond is longer. The C3−N bond has its longest value in vinylamine. It is also seen the C2C1N angle is more bent in APN than in vinyl cyanide. These differences indicate that electron delocalization is considerably more prevalent in APN than in both vinlyamine and vinyl cyanide.

The energy difference[1] between the *Z*- and the *E*-forms of about 8 kJ/mol warrants comments. The effects of electron delocalization should be rather similar in the two forms, so this cannot be the explanation. A major part of the 8 kJ/mol energy difference is perhaps due to intramolecular hydrogen bonding between the nearest hydrogen atom of the amino group (H_s) and the π electrons of the cyano group. This interaction is of course only possible in the *Z*-form.

The internal hydrogen bond in APN is characterized by the following: The nonbonded $H_s\cdots C1$ and $H_s\cdots N$ distances are 252 and 290 pm, respectively (from structure in Table 8), compared to the sum of the van der Waals distances of hydrogen (120 pm)[76] and aromatic carbon (170 pm),[76] which is 290 pm. The distance from H_s to the π electron clouds of the triple bond of the nitrile group is therefore comparatively short.

Moreover, the bond moments of both the C≡N and N−H bonds are relatively large with the nitrogen atoms as the negative end in each case.[77] The C1≡N and N−H_s bonds are calculated to be 7.5° from being parallel, using the structure in Table 8. The bond moments are consequently nearly antiparallel, which is ideal for dipole−dipole stabilization.

Acknowledgment. We thank Anne Horn for her most helpful assistance and George C. Cole for reading the manuscript and correcting and improving the language. A grant from the French-Norwegian Aurora Program to J.-C.G. and H.M. is gratefully acknowledged. The Research Council of Norway (Program for Supercomputing) is thanked for a grant of computer time. J.-C.G. thanks the PCMI (INSU-CNRS) and the CNES for financial support. The Lille group was supported by the Institut du Développement des Ressources en Informatique Scientifique (Contract IDRIS 51715), and by the Program National de Physico-Chimie du Milieu Interstellaire (PCMI).

Supporting Information Available: Preparation procedures of cyanoacetylenes and microwave spectra of the parent molecule and eight isotopologs. This information is available free of charge via the Internet at http://pubs.acs.org.

References and Notes

(1) Benidar, A.; Guillemin, J.-C.; Mó, O.; Yáñez, M. *J. Phys. Chem. A* **2005**, *109*, 4705.
(2) Guillemin, J.-C.; Breneman, C. M.; Joseph, J. C.; Ferris, J. P. *Chem. Eur. J.* **1998**, *4*, 1074.
(3) Xiang, Y.-B.; Drenkard, S.; Baumann, K.; Hickey, D.; Eschenmoser, A. *Helv. Chim. Acta* **1994**, *77*, 2209.
(4) Mann, A. P. C.; Williams, D. A. *Nature (London)* **1980**, *283*, 721.
(5) Ungerechts, H.; Walmsley, C. M.; Winnewisser, G. *Astron. Astrophys.* **1980**, *88*, 259.
(6) Bockelee-Morvan, D.; Lis, D. C.; Wink, J. E.; Despois, D.; Crovisier, J.; Bachiller, R.; Benford, D. J.; Biver, N.; Colom, P.; Davies, J. K.; Gerard, E.; Germain, B.; Houde, M.; Mehringer, D.; Moreno, R.; Paubert, G.; Phillips, T. G.; Rauer, H. *Astron. Astrophys.* **2000**, *353*, 1101.
(7) Kunde, V. G.; Aikin, A. C.; Hanel, R. A.; Jennings, D. E.; Maguire, W. C.; Samuelson, R. E. *Nature (London)* **1981**, *292*, 686.
(8) Coustenis, A.; Encrenaz, T.; Bezard, B.; Bjoraker, G.; Graner, G.; Dang Nhu, M.; Arie, E. *Icarus* **1993**, *102*, 240.
(9) Wyckoff, S.; Tegler, S. C.; Engel, L. *Astrophys. J.* **1991**, *368*, 279.
(10) Huebner, W. F. *Earth, Moon, Planets* **2002**, *89*, 179.
(11) Ksander, G.; Bold, G.; Lattmann, R.; Lehmann, C.; Frueh, T.; Xiang, Y. B.; Inomata, K.; Buser, H. P.; Schreiber, J.; Zass, J.; Eschenmoser, A. *Helv. Chim. Acta* **1987**, *70*, 1115.
(12) Drenkard, S.; Ferris, J.; Eschenmoser, A. *Helv. Chim. Acta* **1990**, *73*, 1373.
(13) Wagner, E.; Xiang, Y. B.; Baumann, K.; Gueck, J.; Eschenmoser, A. *Helv. Chim. Acta* **1990**, *73*, 1391.
(14) Eschenmoser, A. *Origins Life Evol. Biosphere* **1994**, *24*, 389.
(15) Eschenmoser, A.; Loewenthal, E. *Chem. Soc. Rev.* **1992**, *21*, 1.
(16) Curtiss, L. A.; Raghavachari, K.; Trucks, G. W.; Pople, J. A. *J. Chem. Phys.* **1991**, *94*, 7221.
(17) Becke, A. D. *J. Chem. Phys.* **1993**, *98*, 1372.
(18) Lee, C.; Yang, W.; Parr, R. G. *Phys. Rev. B* **1988**, *37*, 785.
(19) Dickens, J. E.; Irvine, W. M.; Nummelin, A.; Møllendal, H.; Saito, S.; Thorwirth, S.; Hjalmarson, A.; Ohishi, M. *Spectrochim. Acta, Part A* **2001**, *57A*, 643.
(20) Bernstein, M. P.; Ashbourn, S. F.; Sandford, S. A.; Allamandola, L. J. *Astrophys. J.* **2004**, *601*, 365.
(21) Hollis, J. T. Personal communication, 2005.
(22) Lovas, F. J.; Clark, F. O.; Tiemann, E. *J. Chem. Phys.* **1975**, *62*, 1925.
(23) Brown, R. D.; Godfrey, P. D.; Kleibömer, B. *J. Mol. Spectrosc.* **1987**, *124*, 21.
(24) Brown, R. D.; Godfrey, P. D.; Kleibömer, B.; Pierlot, A. P.; McNaughton, D. *J. Mol. Spectrosc.* **1990**, *142*, 195.
(25) Ammonia-^{15}N (10% isotopic purity) purchased from Aldrich was used to minimize the cost. Thus, all the ^{15}N-products (cyanoacetylene-^{15}N,

both isotopomers of aminopropenenitrile-^{15}N and amino-^{15}N-propenenitrile) have a 10% isotopic purity.

(26) Møllendal, H.; Leonov, A.; de Meijere, A. *J. Phys. Chem. A* **2005**, *109*, 6344.

(27) Møllendal, H.; Cole, G. C.; Guillemin, J.-C. *J. Phys. Chem. A* **2006**, *110*, 921.

(28) Kassi, S.; Petitprez, D.; Wlodarczak, G. *J. Mol. Struct.* **2000**, *517*−*518*, 375.

(29) Helgaker, T.; Gauss, J.; Jørgensen, P.; Olsen, J. *J. Chem. Phys.* **1997**, *106*, 6430.

(30) Møller, C.; Plesset, M. S. *Phys. Rev.* **1934**, *46*, 618.

(31) Watson, J. K. G. *Vibrational Spectra and Structure*; Elsevier: Amsterdam, 1977; Vol. 6.

(32) Frisch, M. J.; Trucks, G. W.; Schlegel, H. B.; Scuseria, G. E.; Robb, M. A.; Cheeseman, J. R.; Montgomery, J. A., Jr.; Vreven, T.; Kudin, K. N.; Burant, J. C.; Millam, J. M.; Iyengar, S. S.; Tomasi, J.; Barone, V.; Mennucci, B.; Cossi, M.; Scalmani, G.; Rega, N.; Petersson, G. A.; Nakatsuji, H.; Hada, M.; Ehara, M.; Toyota, K.; Fukuda, R.; Hasegawa, J.; Ishida, M.; Nakajima, T.; Honda, Y.; Kitao, O.; Nakai, H.; Klene, M.; Li, X.; Knox, J. E.; Hratchian, H. P.; Cross, J. B.; Adamo, C.; Jaramillo, J.; Gomperts, R.; Stratmann, R. E.; Yazyev, O.; Austin, A. J.; Cammi, R.; Pomelli, C.; Ochterski, J. W.; Ayala, P. Y.; Morokuma, K.; Voth, G. A.; Salvador, P.; Dannenberg, J. J.; Zakrzewski, V. G.; Dapprich, S.; Daniels, A. D.; Strain, M. C.; Farkas, O.; Malick, D. K.; Rabuck, A. D.; Raghavachari, K.; Foresman, J. B.; Ortiz, J. V.; Cui, Q.; Baboul, A. G.; Clifford, S.; Cioslowski, J.; Stefanov, B. B.; Liu, G.; Liashenko, A.; Piskorz, P.; Komaromi, I.; Martin, R. L.; Fox, D. J.; Keith, T.; Al-Laham, M. A.; Peng, C. Y.; Nanayakkara, A.; Challacombe, M.; Gill, P. M. W.; Johnson, B.; Chen, W.; Wong, M. W.; Gonzalez, C.; Pople, J. A. *Gaussian 03*, Revision B.03; Gaussian, Inc.: Pittsburgh, PA, 2003.

(33) Ray, B. S. *Z. Physik* **1932**, *78*, 74.

(34) Sørensen, G. O. ROTFIT. Personal communication, 1972.

(35) Gordy, W.; Cook, R. L. *Microwave Molecular Spectra*; Techniques of Chemistry, Vol. 18; John Wiley & Sons: New York, 1984.

(36) Pickett, H. M. *J. Mol. Spectrosc.* **1991**, *148*, 371.

(37) Laurie, V. W.; Herschbach, D. R. *J. Chem. Phys.* **1962**, *37*, 1687.

(38) Esbitt, A. S.; Wilson, E. B. *Rev. Sci. Instrum.* **1963**, *34*, 901.

(39) Muenter, J. S. *J. Chem. Phys.* **1968**, *48*, 4544.

(40) Golden, S.; Wilson, E. B., Jr. *J. Chem. Phys.* **1948**, *16*, 669.

(41) Marstokk, K.-M.; Møllendal, H. *J. Mol. Struct.* **1969**, *4*, 470.

(42) Costain, C. C. *J. Chem. Phys.* **1958**, *29*, 864.

(43) Kraitchman, J. *Am. J. Phys.* **1953**, *21*, 17.

(44) Costain, C. C. *Trans. Am. Crystallogr. Assoc.* **1966**, *2*, 157.

(45) Van Eijck, B. P. *J. Mol. Spectrosc.* **1982**, *91*, 348.

(46) Margulès, L.; Demaison, J.; Boggs, J. E. *J. Mol. Struct. (THEOCHEM)* **2000**, *500*, 245.

(47) Margulès, L.; Demaison, J.; Boggs, J. E. *Struct. Chem.* **2000**, *11*, 145.

(48) Margulès, L.; Demaison, J.; Rudolph, H. D. *J. Mol. Struct.* **2001**, *599*, 23.

(49) Purvis, G. D., III.; Bartlett, R. J. *J. Chem. Phys.* **1982**, *76*, 1910.

(50) Raghavachari, K.; Trucks, G. W.; Pople, J. A.; Head-Gordon, M. *Chem. Phys. Lett.* **1989**, *157*, 479.

(51) Kohn, W.; Sham, L. J. *Phys. Rev.* **1965**, *140*, 1133.

(52) Becke, A. D. *J. Chem. Phys.* **1993**, *98*, 5648.

(53) Curtiss, L. A.; Raghavachari, K.; Redfern, P. C.; Rassolov, V.; Pople, J. A. *J. Chem. Phys.* **1998**, *109*, 7764.

(54) Dunning, T. H., Jr. *J. Chem. Phys.* **1989**, *90*, 1007.

(55) Demaison, J.; Császár, A. G.; Kleiner, I.; Møllendal, H. To be submitted for publication.

(56) Kendall, R. A.; Dunning, T. H., Jr.; Harrison, R. J. *J. Chem. Phys.* **1992**, *96*, 6796.

(57) Császár, A. G.; Allen, W. D. *J. Chem. Phys.* **1996**, *104*, 2746.

(58) Peterson, K. A.; Dunning, T. H., Jr. *J. Chem. Phys.* **2002**, *117*, 10548.

(59) Basis sets were obtained from the Extensible Computational Chemistry Environment Basis Set Database, Version 6/19/03, as developed and distributed by the Molecular Science Computing Facility, Environmental and Molecular Sciences Laboratory, which is part of the Pacific Northwest Laboratory Richland, WA, and funded by the U.S. Department of Energy. The Pacific Northwest Laboratory is a multi-program laboratory operated by Battelle Memorial Institute for the U.S. Department of Energy under Contract DE-AC06-76RLO 1830. Contact David Feller or Karen Schuchardt for further information.

(60) Werner, H.-J.; Knowles, P. J.; Amos, R. D.; Berhardsson, A.; Berning, A.; Celani, P.; Cooper, D. L.; Degan, M. J. O.; Dobbyn, A. J.; Eckert, F.; Hampel, C.; Hetzer, G.; Lindh, R.; Lloyd, A. W.; McNicholas, S. J.; Manby, F. R.; Meyer, W.; Mura, M. E.; Nicklass, A.; Palmieri, P.; Pitzer, R.; Rauhut, G.; Schütz, M.; Stoll, H.; Stone, A. J.; Tarroni, R.; Thorsteinsson, T. *MOLPRO*; University College Cardiff Consultants, Ltd.: Cardiff, U.K., 2000.

(61) Hampel, C.; Peterson, K. A.; Werner, H. J. *Chem. Phys. Lett.* **1992**, *190*, 1.

(62) Deegan, M. J. O.; Knowles, P. J. *Chem. Phys. Lett.* **1994**, *227*, 321.

(63) Demaison, J.; Cosléou, J.; Bocquet, R.; Lesarri, A. G. *J. Mol. Spectrosc.* **1994**, *167*, 400.

(64) Colmont, J. M.; Wlodarczak, G.; Priem, D.; Müller, H. S. P.; Tien, E. H.; Richards, R. J.; Gerry, M. C. L. *J. Mol. Spectrosc.* **1997**, *181*, 330.

(65) Harmony, M. D.; Taylor, W. H. *J. Mol. Spectrosc.* **1986**, *118*, 163.

(66) Lee, T. J.; Taylor, P. R. *Int. J. Quantum Chem., Quantum Chem. Symp.* **1989**, *23*, 199.

(67) Halter, R. J.; Fimmen, R. L.; McMahon, R. J.; Peebles, S. A.; Kuczkowski, R. L.; Stanton, J. F. *J. Am. Chem. Soc.* **2001**, *123*, 12353.

(68) Kissel, J.; Krueger, F. R. *Nature (London)* **1987**, *326*, 755.

(69) McNaughton, D.; Evans, C. J. *J. Mol. Spectrosc.* **1999**, *196*, 274.

(70) Pillsbury, N. R.; Drucker, S. *J. Mol. Spectrosc.* **2004**, *224*, 188.

(71) Margulès, L.; Demaison, J.; Boggs, J. E. *J. Phys. Chem. A* **1999**, *103*, 7632.

(72) Lesarri, A. G.; Cosléou, J.; Li, X.; Wlodarczak, G.; Demaison, J. *J. Mol. Spectrosc.* **1995**, *172*, 520.

(73) Omron, R. M.; Hight Walker, A. R.; Hilpert, G.; Fraser, G. T.; Suenram, R. D. *J. Mol. Spectrosc.* **1996**, *179*, 85.

(74) Dimitrova, V.; Ilieva, S.; Galabov, B. *J. Phys. Chem. A* **2002**, *106*, 11801.

(75) Herbst, E.; Klemperer, W. *Phys. Today* **1976**, *29*, 32.

(76) Pauling, L. *The Nature of the Chemical Bond*; Cornell University Press: New York, 1960.

(77) Smyth, C. P. *Dielectric Behavior and Structure*; McGraw-Hill: New York, 1955.